



Analysis of carbon-bearing materials for use as first wall armor in the HAPL chamber

T.A. Heltemes and G.A. Moses, Fusion Technology Institute

BUCKY Simulations of gas-filled chambers can be used to predict the thermal response of armor materials

Abstract

The characterization of lifetime-component capabilities of various chamber armors is a critical path to the development of the HAPL reactor design. Previous studies have examined tungsten as an armor material to protect the low-activation ferritic steel first wall from x-ray and ion damage.

Carbon-bearing materials are of interest as candidate armor materials due to their desirable thermal and mechanical properties. This analysis examines and compares several carbon-bearing materials: silicon carbide, graphite, engineered graphitic materials and carbon nanotube composites.

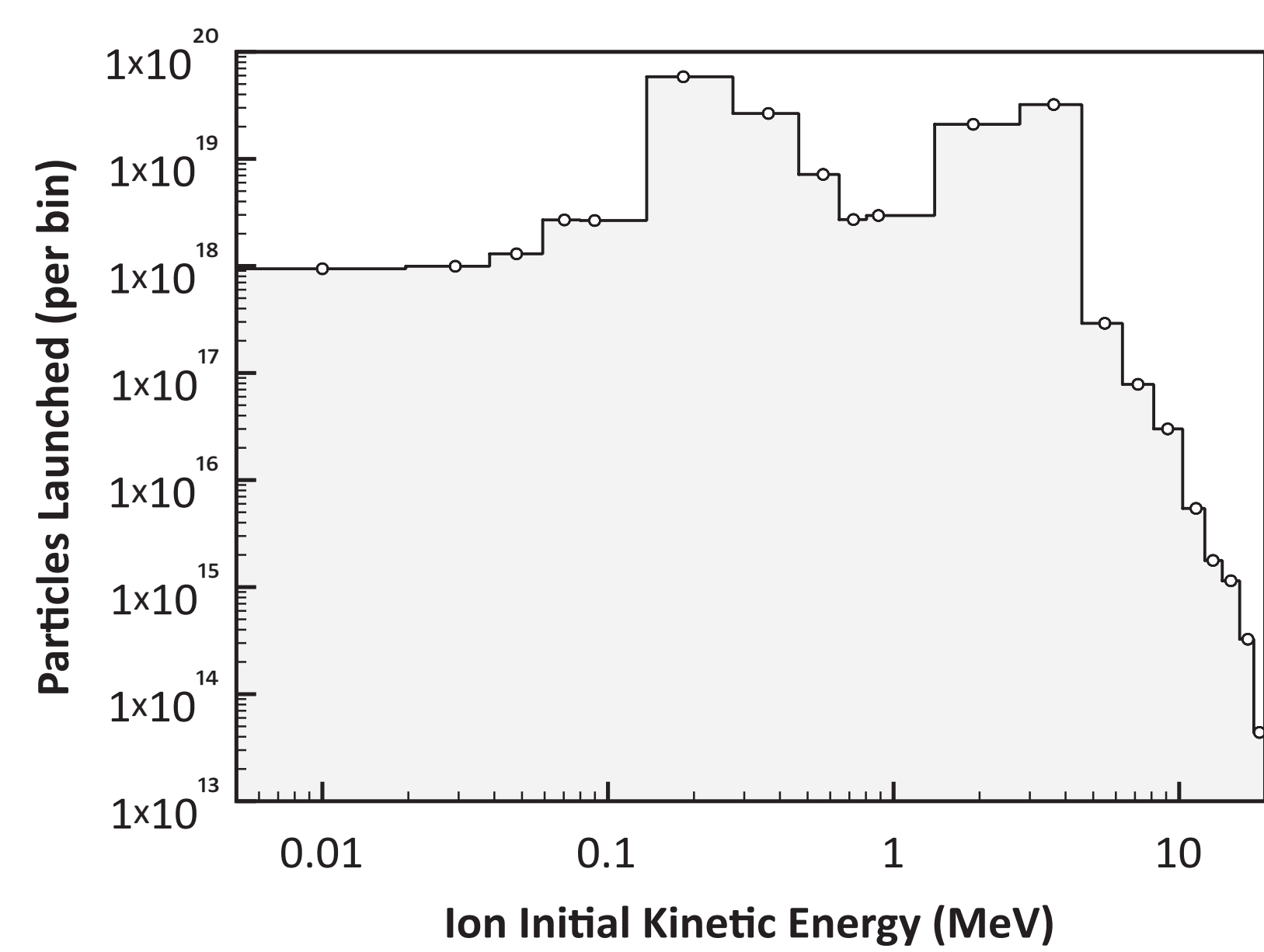
The transient thermal response of these materials was simulated with the BUCKY 1-D radiation hydrodynamics code utilizing the standardized HAPL x-ray and ion threat spectra. Evacuated and buffer gas filled bare-walled configurations were simulated.

BUCKY Simulation Setup

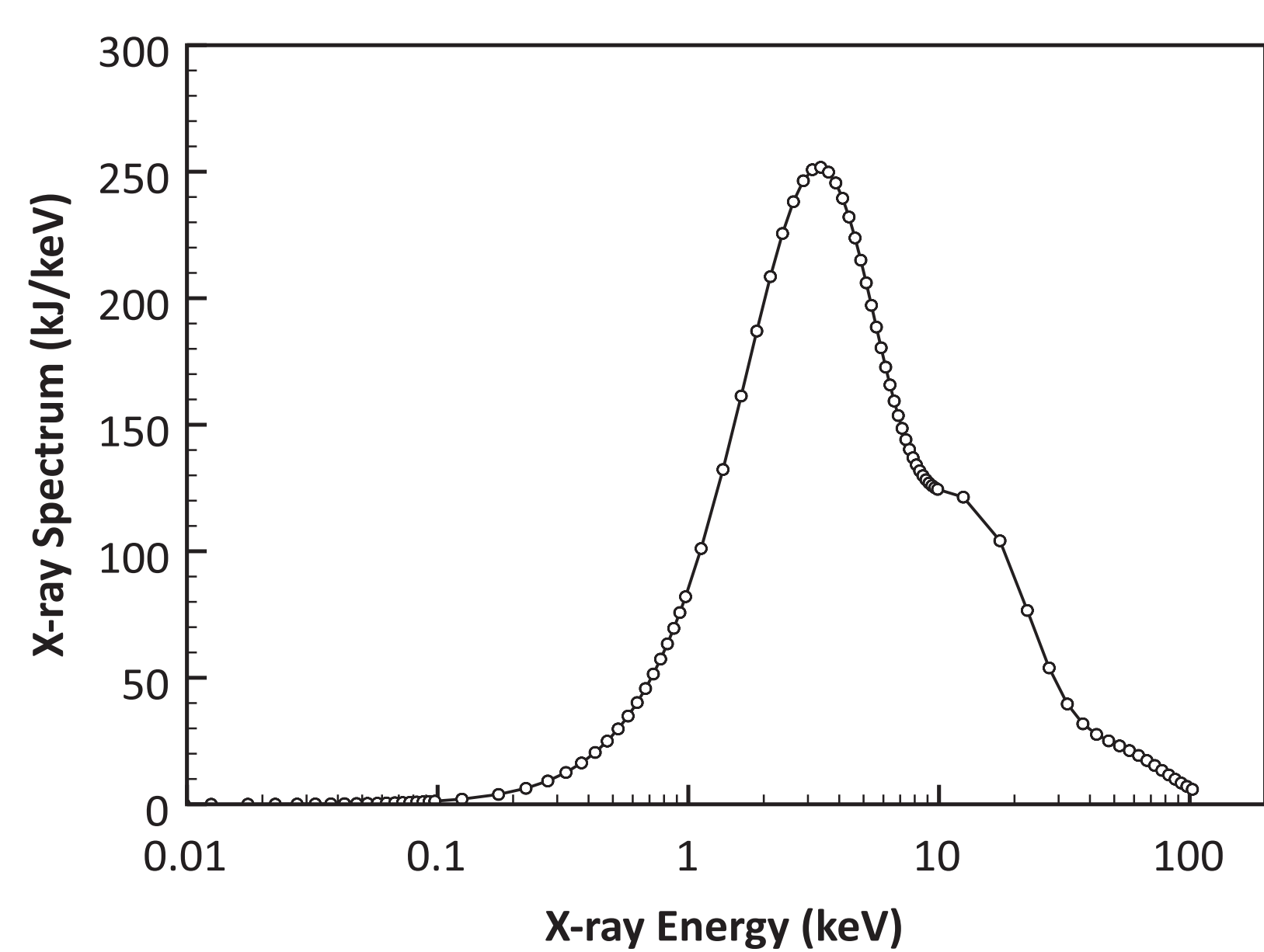
The BUCKY simulations were set up with the following initial conditions:

- * Chamber radius of 10.5 meters with helium gas fills of 0.5 mtorr and 11.6 mtorr at 600 °C and initial wall material temperature of 600 °C.
- * All ions are launched simultaneously at the beginning of the simulation ($t = 0$ s). For clarity, only the HAPL target alpha ion spectrum is shown here — the complete ion source spectral data appear in Reference 1.
- * The start of the time-dependent x-ray pulse is concurrent with the launch of the ions ($t = 0$ s). The x-ray pulse intensity is modeled as a gaussian distribution with a full-width half-maximum of 170 ps¹. The x-ray pulse ends at 750 ps.
- * 2-T SESAME equation-of-state data were used for the helium gas in the chamber². YAC non-LTE opacities are used for radiation transport for all materials³.
- * Thermal conductivity and specific heat data for tungsten were obtained from the NIST Standard Reference Database^{4,5}. Graphite specific heat and thermal conductivity data were obtained from the NIST Standard Reference Database^{5,6}. Silicon carbide thermal conductivity and specific heat data were obtained from the ITER Material Properties Handbook⁷.

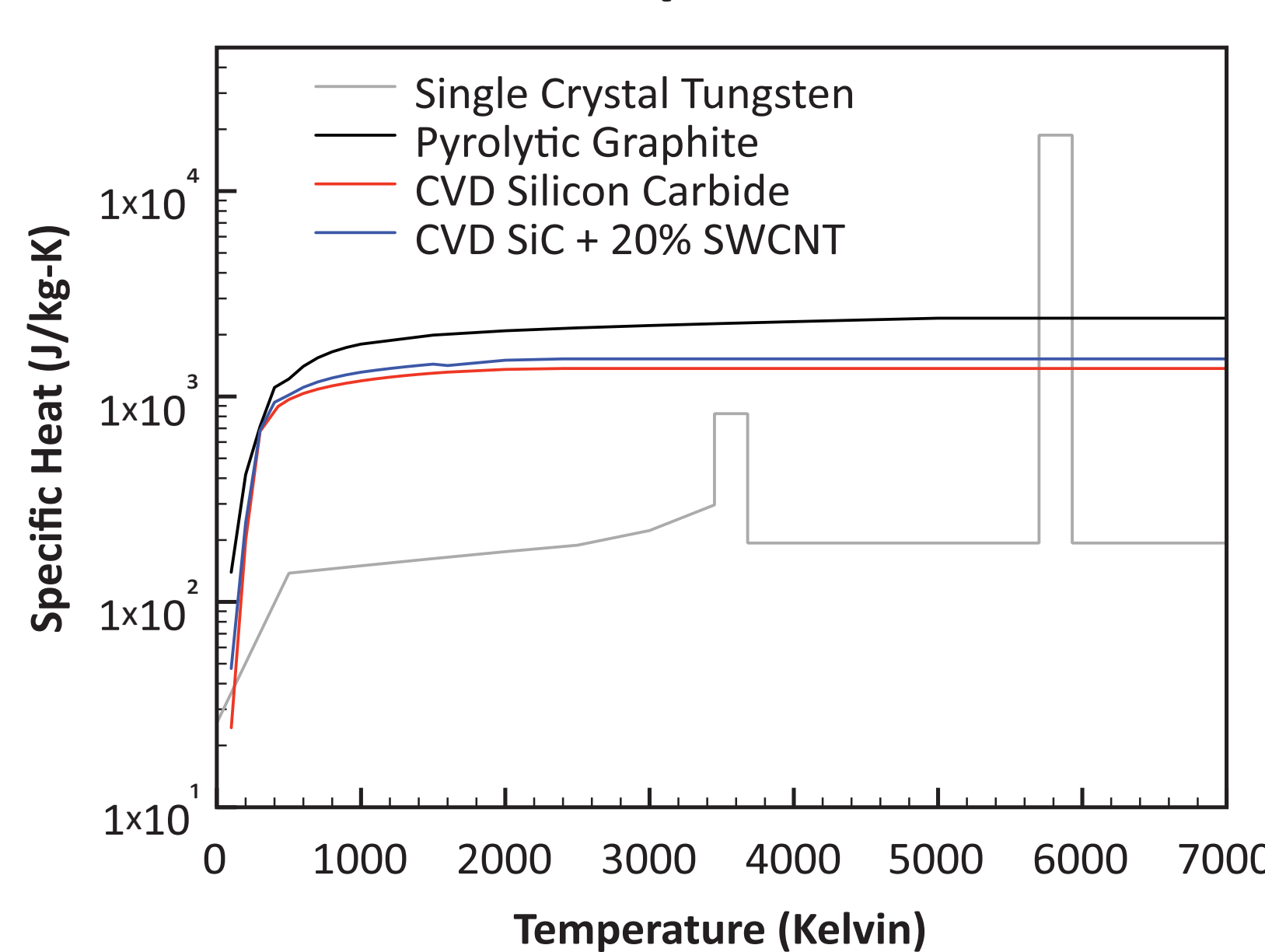
HAPL alpha spectrum, as launched



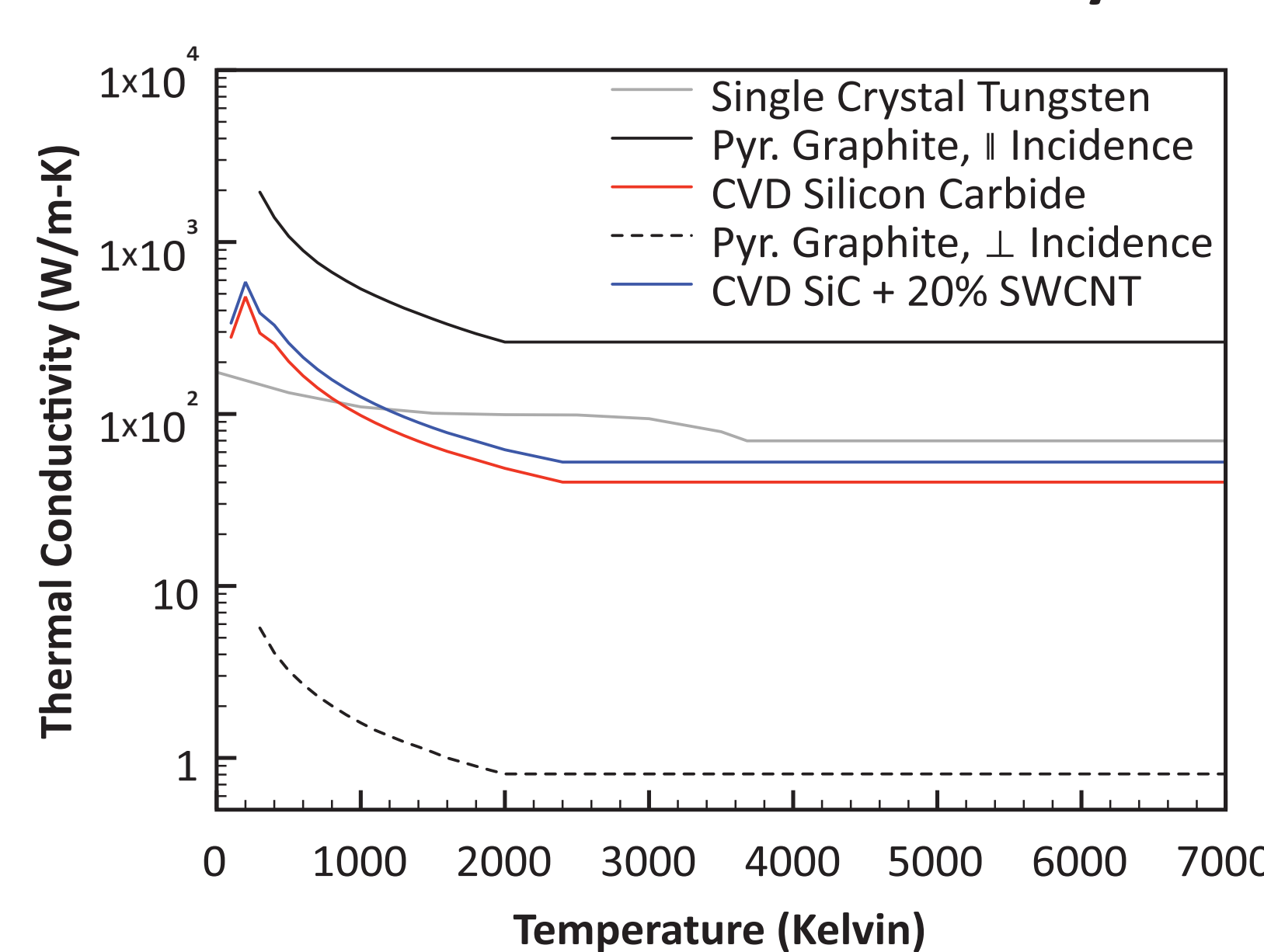
HAPL x-ray spectrum, as launched



Armor material specific heat data



Armor material thermal conductivity data



The results of the simulations demonstrate that simplistic estimates of temperature responses are not appropriate

Previous research efforts have focused on the surface temperature response and lifetime estimates for tungsten armor protecting a low-activation ferritic steel first wall¹. The tungsten results will be reproduced here to provide a basis for comparison with the carbon-bearing material simulation results.

All simulations presented here assume that materials are in the unirradiated state.

CVD Silicon Carbide

Chemical vapor deposition (CVD) silicon carbide with <10 μm grain size was simulated. This material configuration was chosen because of the isotropic nature of the thermal conductivity data available.

Pyrolytic Graphite

Two pyrolytic graphite simulations were performed: (1) one with the incident ions and x-rays parallel to the graphite planes and (2) a second with the incident ions and x-rays perpendicular to the graphite planes — resulting in the best- and worst-case scenarios due to the anisotropic nature of the thermal conductivity of graphite.

Carbon Nanotube Reinforced Composite

The carbon nanotube reinforced composite examined was composed of single-walled carbon nanotubes (SWCNT) with random orientation embedded in a CVD silicon carbide matrix. A simple mixing model was used to calculate the temperature-dependent thermal conductivity and specific heat data^{9,10}.

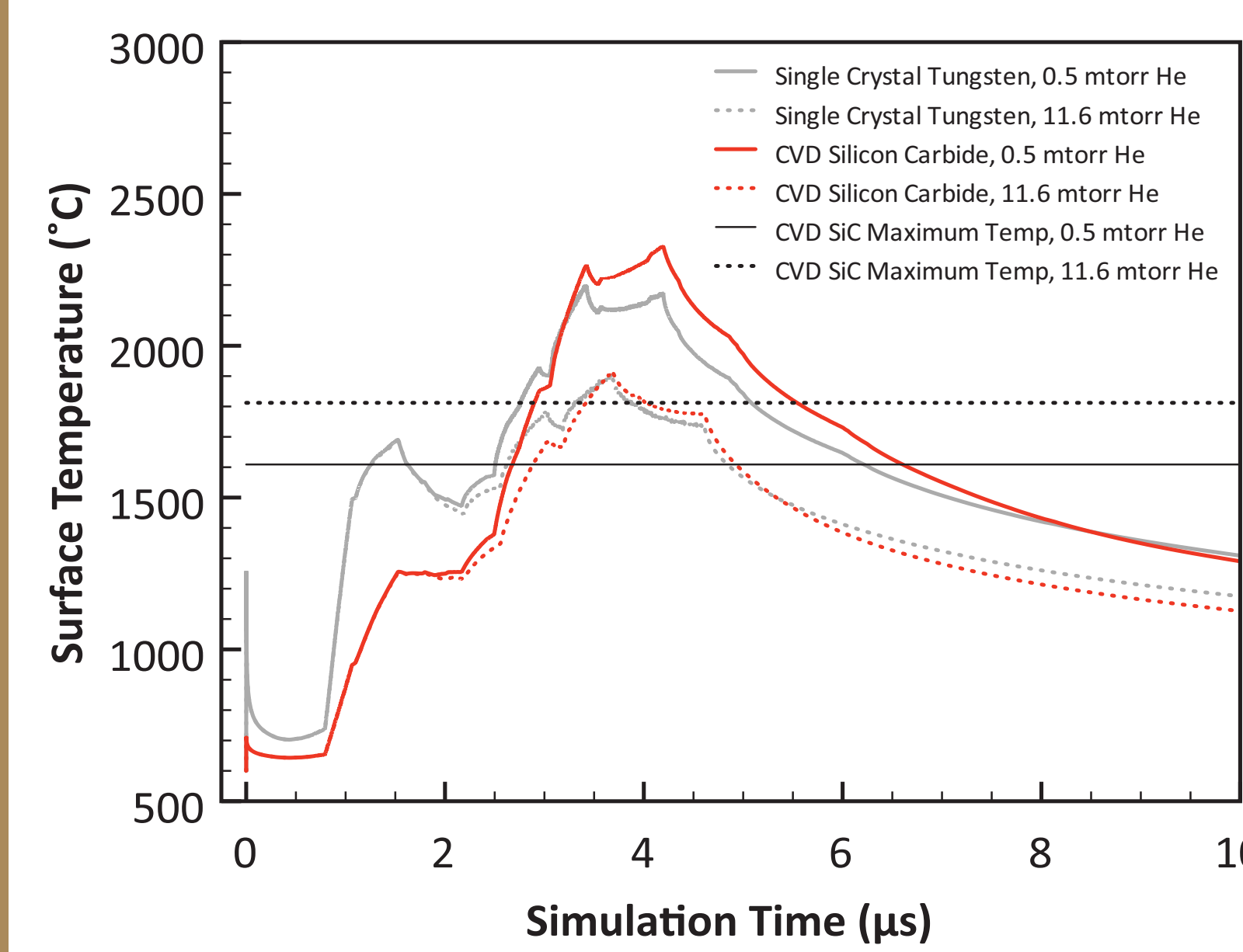
The composite modeled assumed a mass fraction of 20% carbon nanotubes and the remaining 80% consisting of CVD silicon carbide.

Engineered Graphite Surface (ESLI Carbon Spike)

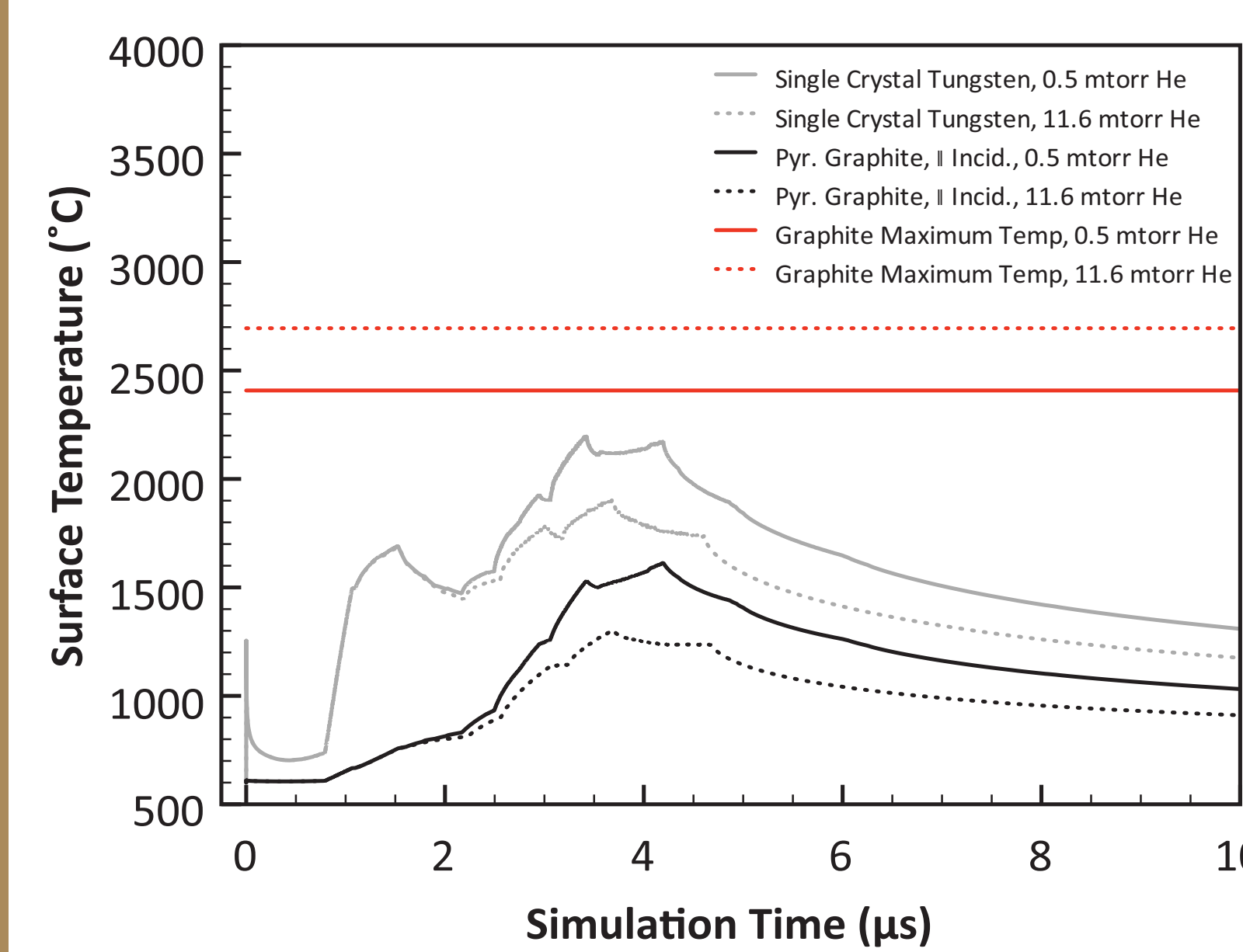
The engineered graphite wall analyzed was the ESLI carbon spike sheet model⁸. The chamber first wall would be lined with a graphite substrate to which a layer of carbon spikes would be attached. An individual spike is 1 mm long with a 35 μm diameter base.

For this analysis, the spikes were arranged in a perpendicular grid with the bases in contact with each other. This configuration results in a surface area multiplication of ~328.5 over that of a smooth graphite armor surface.

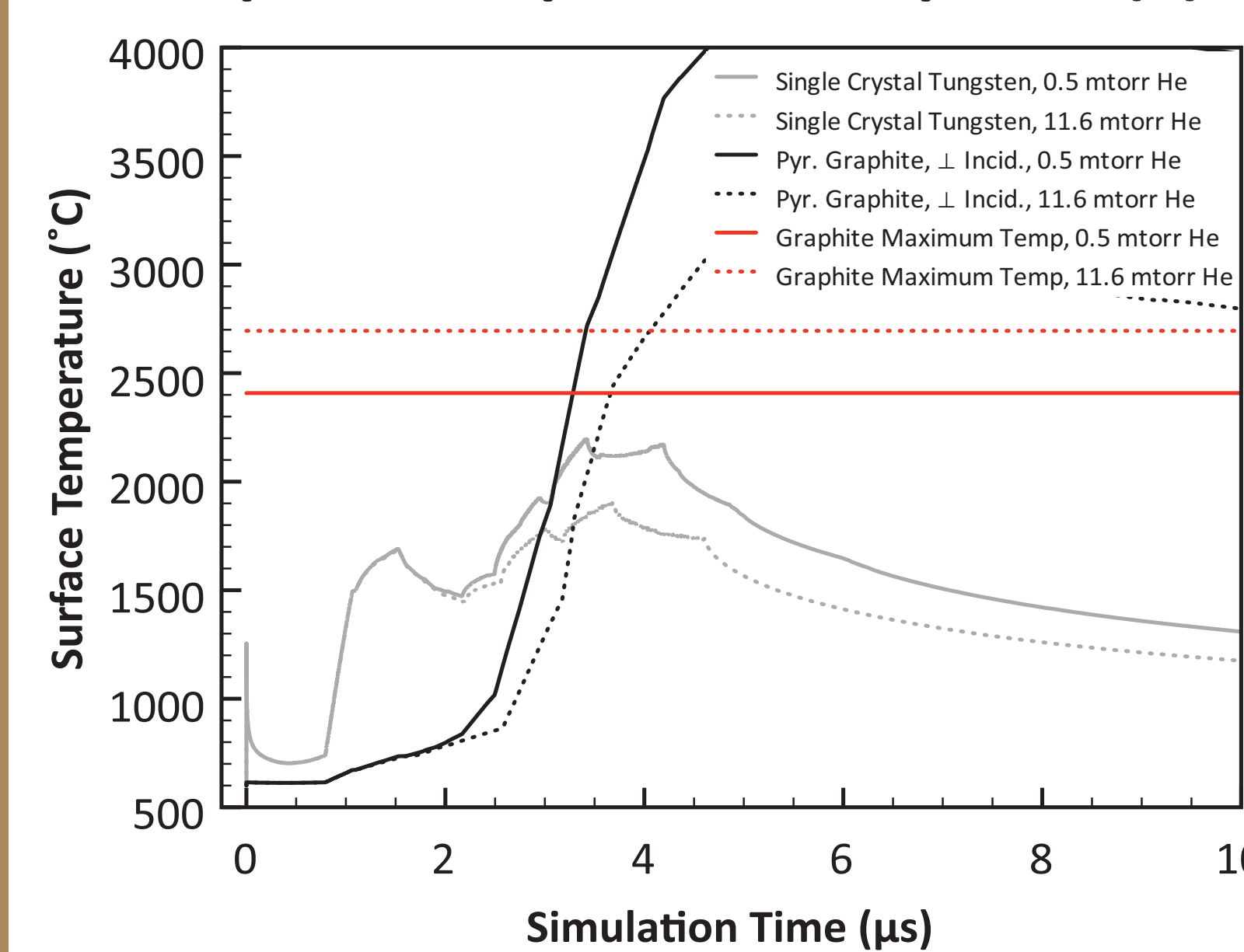
Silicon carbide temperature response



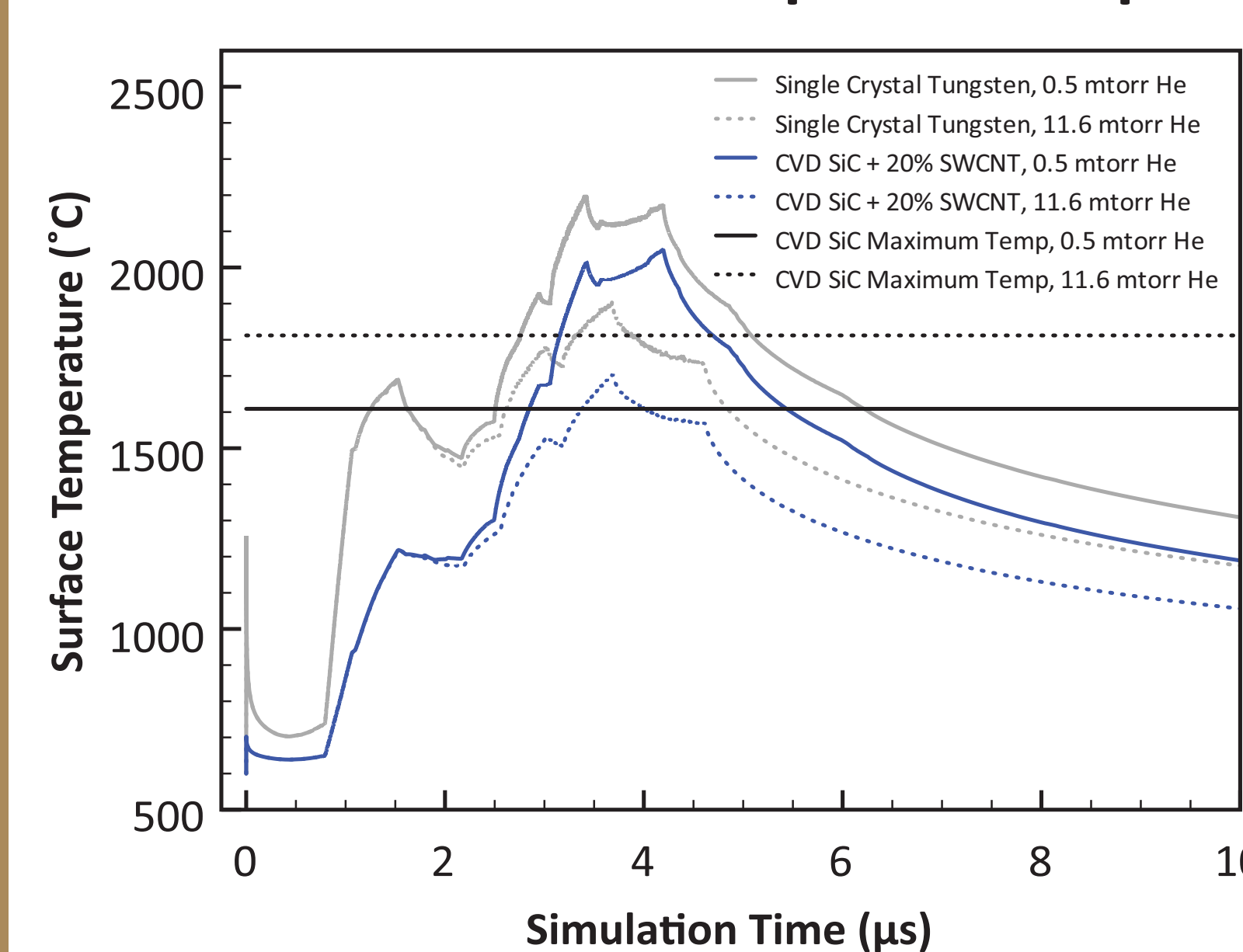
Graphite temperature response (1)



Graphite temperature response (2)



CVD SiC + 20% SWCNT temperature response



The use of engineered carbon materials and carbon nanotube composites are promising and require further analysis

Because the threat spectra angle-of-incidence of the surface of the spike changes as the impact point is moved down the shaft of the spike, a parametric set of simulations were performed to ascertain the location-dependent temperature profile. This was accomplished by examining a differential area element and scaling the source intensity by the sine of the angle-of-incidence (which is 90° — normal incidence — at the tip of the carbon spike). A semi-logarithmic selection of distances from the tip of the spike (0 μm) to 10 μm from the tip were simulated. Incident ion and x-ray threat spectra are assumed to be parallel to the graphite planes. Chamber helium gas pressures of (1) 0.5 mtorr and (2) 11.6 mtorr at 600 °C were simulated.

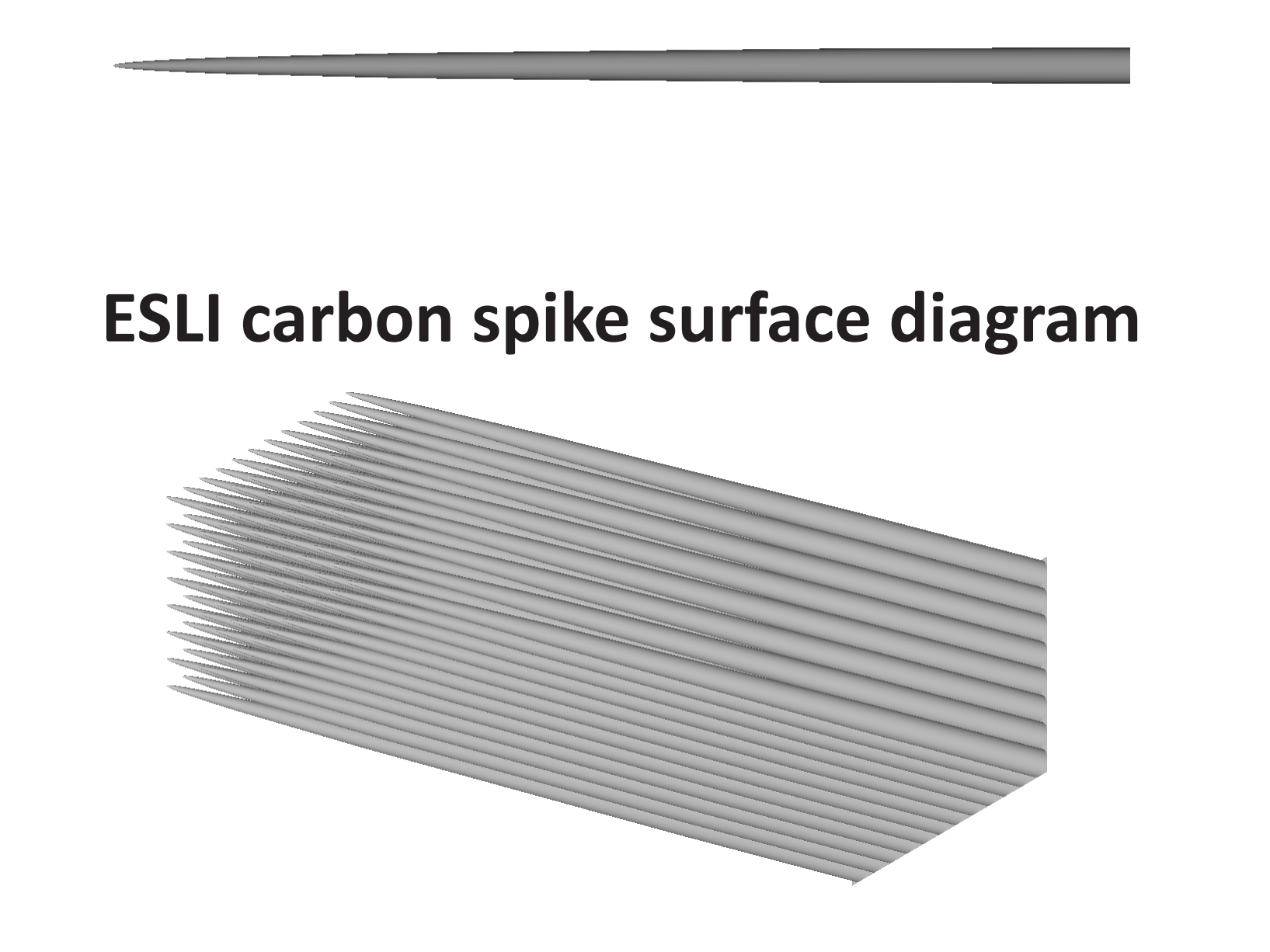
Acknowledgement

This work supported in part by a grant from the Naval Research Laboratory, award no. N00173-03-1-G901.

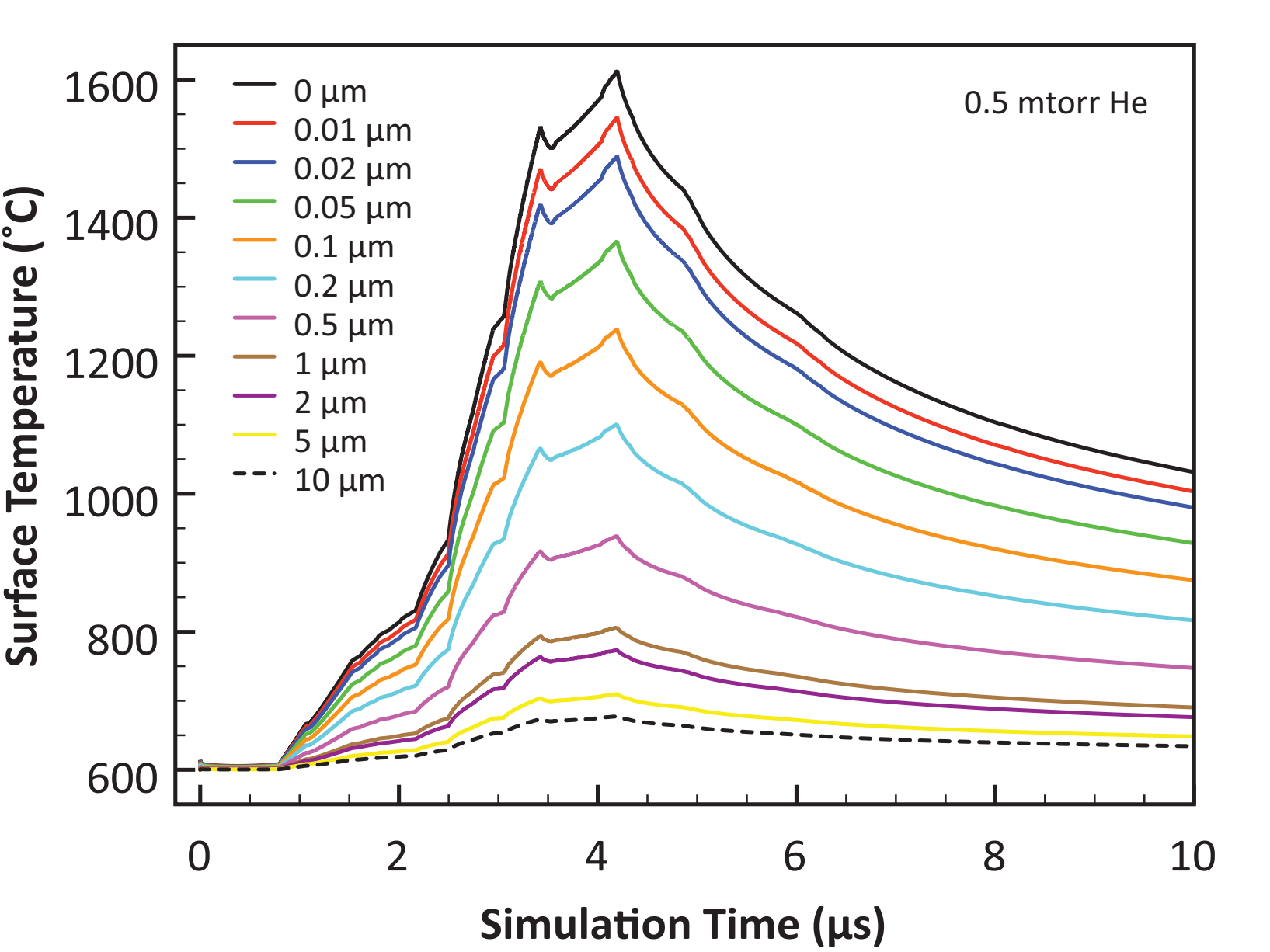
References

1. T.A. Heltemes, D.R. Boris, G.A. Moses and M. Fatenejad, "Simulation of thermal response and ion deposition in the HAPL target chamber 1 mm tungsten armor layer using the improved BUCKY code", *Fusion Engineering and Design* 82(2), pp. 175-187 (2007).
2. B.I. Bennet, J.D. Johnson, G.I. Kerley and G.T. Rood, "Recent Developments in the SESAME Equation-of-State Library", Los Alamos National Laboratory, NM, LA-7130 (1978).
3. J. Yuan, D.A. Haynes, R.R. Peterson and G.A. Moses, "Flexible database-driven opacity and spectrum calculations", *J. Quant. Spect. Rad. Trans.* 81, 513 (2003).
4. Strem Chemicals, Catalog No. 18, Strem Chemicals, Newburyport, MA, 1999, 418. Data reported in NIST Standard Reference Database 69, Release: NIST Chemistry WebBook (June 2005).
5. M.W. Chase Jr., NIST-JANAF Thermochemical Tables, fourth ed., Data reported in NIST Standard Reference Database 69, *J. Phys. Chem. Ref. Data, Monograph* 9, pp. 1-1951, Release: NIST Chemistry WebBook, (June 2005).
6. C.Y. Ho, R.W. Powell and P.E. Liley, "Thermal Conductivity of the Elements: A Comprehensive Review", *J. Phys. Chem. Ref. Data* 3(1), pp. 1-756 (1974).
7. L.L. Snead, T. Nozawa, Y. Katoh, T.S. Byun, S. Kondo and D.A. Petti, "Handbook of SiC properties for fuel performance modeling", *Journal of Nuclear Materials* 371, pp. 329-377 (2007).
8. C.A. Seaman and T.R. Knowles, "Carbon Velvet Thermal Interface Gaskets", 39th AIAA Aerospace Sciences Meeting, Reno, NV, AIAA-2001-0217 (2001).
9. C.W. Nan, Z. Shi and Y. Lin, "A simple model for thermal conductivity of carbon nanotube-based composites", *Chemical Physics Letters* 375, pp. 666-669 (2003).
10. J. Hone, M.C. Laguno, M.J. Bierck, A.T. Johnson, B. Batlogg, Z. Benes and J.E. Fischer, "Thermal properties of carbon nanotubes and nanotube-based materials", *App. Phys. A* 74, pp. 339-343 (2002).

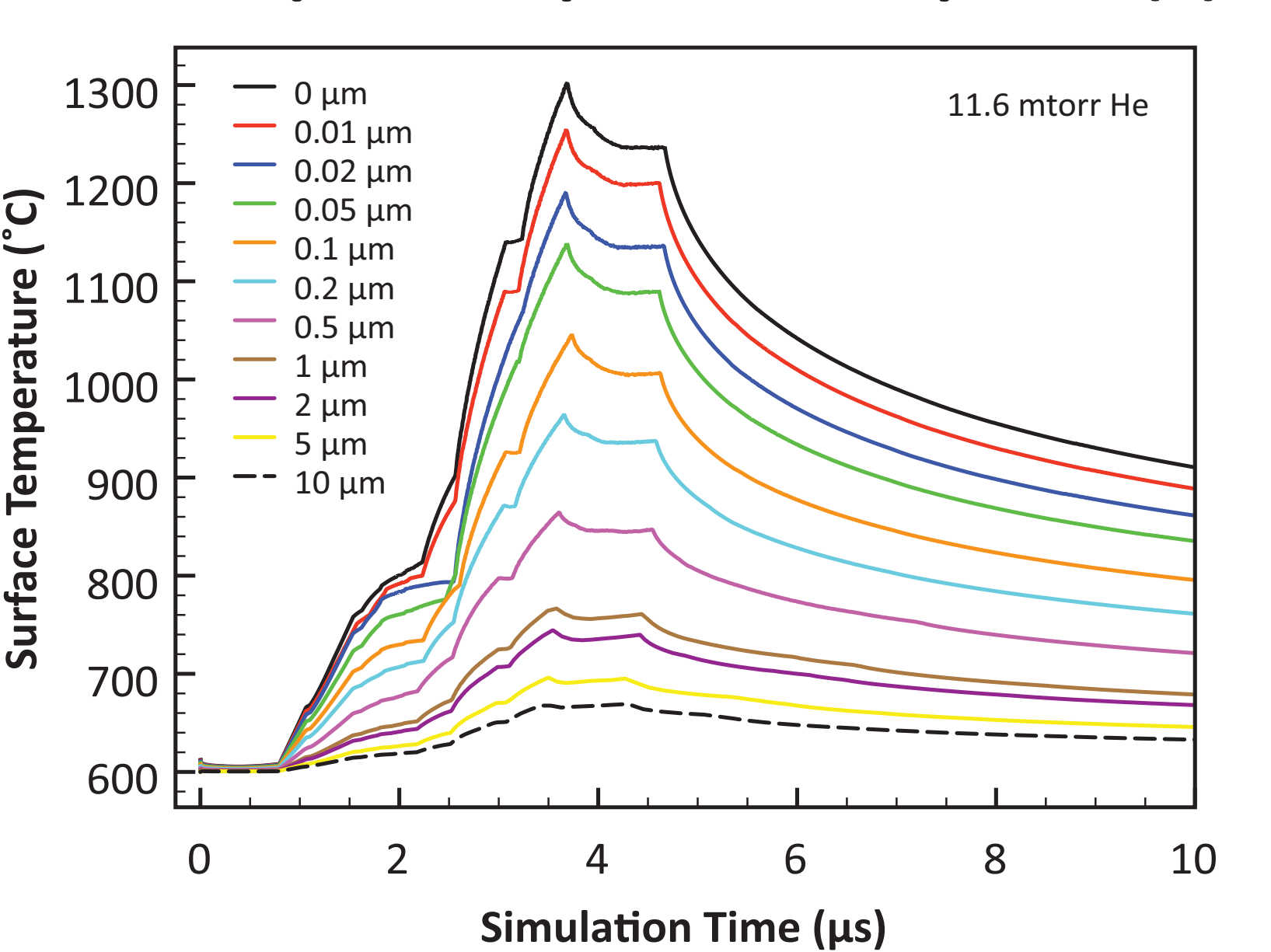
ESLI individual carbon spike diagram



Carbon spike temperature response (1)



Carbon spike temperature response (2)



Summary of 0.5 mtorr He temperature response data

